[SSC20-S2-16]

GaN-Based, Ultra-Compact Power Conversion System for the PUFFER Autonomous Mobility Platform

Ansel Barchowsky, Ahmadreza Amirahmadi, Diego Santillan, Andy Burkic, Jessica Loveland, Autumn Lui, Jaqueline Rapinchuk, Louis Freitas, Chris Stell, Kalind Carpenter
Jet Propulsion Laboratory, California Institute of Technology
4800 Oak Grove Dr, Pasadena, CA 91109
ansel.barchowsky@jpl.nasa.gov

Sadab Mahmud, William Collings, Roshan Kini, Ahmad Javaid, Raghav Khanna
University of Toledo
2801 West Bancroft Street, Toledo, OH 43606; (419)5308183
sadab.mahmud@utoledo.edu

Xavier Zapien
Massachusetts Institute of Technology
77 Massachusetts Ave, Cambridge, MA 02139
xzapien@mit.edu

ABSTRACT

In the pursuit for the development of small rovers for planetary science missions, there is a distinct need for the development of an advanced, autonomously controlled, power subsystem. Existing bus management systems used in large spacecraft missions are not suitable for small spacecraft missions, as they are massive, relatively inefficient, and expensive. For extremely compact rover mission concept, newly developed high-density, high-efficiency, lightweight, and low-cost electronics are required. This paper presents a radiation-hardened power subsystem for the Pop-Up Flat-Folding Explorer Robot (PUFFER) mission concept, utilizing GaN-based converters for solar array conversion, battery management, and point of load applications to provide an extremely compact power subsystem.

INTRODUCTION

The Pop-Up Flat-Folding Explorer Robot (PUFFER) is a small two-wheeled expanding rover designed for swarm surface mobility on planetary bodies throughout the solar system [1]. In a total spacecraft volume of 650 cm^3, mass of 1.18 kg, and usable surface area of 130 cm^2, it represents one of the most compact mobility platforms ever developed for deep-space planetary surface missions. Because of that extremely compact form-factor, the entire power system, including solar arrays, batteries, and power conversion, is extremely limited in mass, volume, and capacity. These extreme limits require a power subsystem that provides 50 W at greater than 95% efficiency, 2 W/cm^3 power density, and 1000 W/kg specific power.

In order to meet the efficiency, power density, and specific power targets for the subsystem, a digitally controlled, Gallium Nitride (GaN)-based, buck-boost converter has been developed, along with supporting conversion for point of load and instrument applications. The subsystem consists of a four-switch GaN-based buck-boost converter processing 10 – 16 V photovoltaic (PV) array power to an unregulated 8 – 12 V battery bus at 95% efficiency. Optimal performance on the solar array is achieved using an Adaptive Ripple Correlation Control-based Maximum Power Point Tracking (MPPT), utilizing Ripple Correlation Control to achieve minimal disturbance on the power system, and implemented in a radiation-hardened ARM M0+ Cortex [2], [3]. Down-conversion to 5 V and 3.3 V busses are achieved with integrated radiation-tolerant point of load modules at 93% efficiency. Instrument power conversion is achieved with a GaN-based boost converter to a 28 V ground-penetrating radar system at 97% efficiency. Telemetry for the power subsystem is collected locally and communicated to the spacecraft avionics platform via serial peripheral interface (SPI). The complete subsystem is housed on a rigid-flex PCB with total dimensions 5cm x 3cm x2 cm 0.075 kg.

The result of this development and testing is a new ultra-compact power subsystem that will provide PUFFER and other small mobility platforms with a radiation-tolerant, high-density, and high-efficiency solution for their power-conversion needs. Future validation on the Lunar surface will demonstrate the system in environments for the lunar surface and beyond.

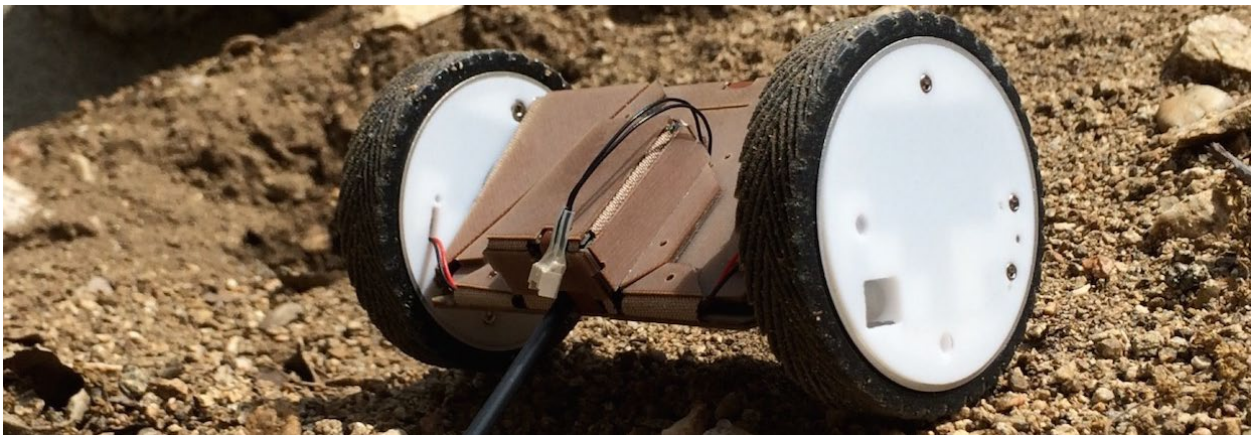

Figure 1. Prototype PUFFER in regolith testbed

PUFFER POWER SYSTEM ARCHITECTURE

The PUFFER is an extremely compact mobility platform, a prototype for which can be seen in Fig. 1., minimizing conversion and telemetry elements to reduce board area and thermal losses. To meet these goals, the power system architecture shown in Fig. 2 has been developed. This section will describe each element briefly, followed by detailed discussions on each element in the following sections. Table 1 provides a specification on each key power bus within the subsystem. This section describes the power conversion needs for each of the subsystem buses in brief, will full specifications for each, including architecture and efficiency measurements in subsequent sections.

Table 1: PUFFER System Specifications

Parameter	Voltage Range	Current Range
PV Array	10 – 15 V	0 – 1 A
Battery Bus	8 – 12 V	0 – 5 A
5V Instrument Bus	5 V	0 – 2 A
3.3V Instrument Bus	3.3 V	0 – 2 A
28 V GPR Bus	24 V	0 – 0.5 A

Photovoltaic Buck-Boost Converter

PUFFER utilizes a PV generation system, coupled with an unregulated battery bus. To maximize efficiency from the PV array to the battery bus, a four-switch buck-boost converter utilizing an RCC MPPT algorithm to set the bus voltage as appropriate to charge the battery while pushing the array to its MPP. The 12V unregulated bus voltage moves with the state of charge of the battery, and all loads are compliant with the wide battery range.

Point of Load (PoL) Converters

Compute element, telemetry, and instrument loads on PUFFER require 5 V and 3.3 V rails. To meet these needs, the architecture utilizes two FET-integrated PoL modules, along with integrated flight system telemetry circuitry to monitor voltage and current.

Ground Penetrating Radar Boost Converter

The primary instrument on one PUFFER variant is a GPR, requiring a 24 V rail for operation. To meet that need, the system utilizes a GaN-based synchronous boost converter with integrated flight system telemetry circuit to monitor voltage and current.

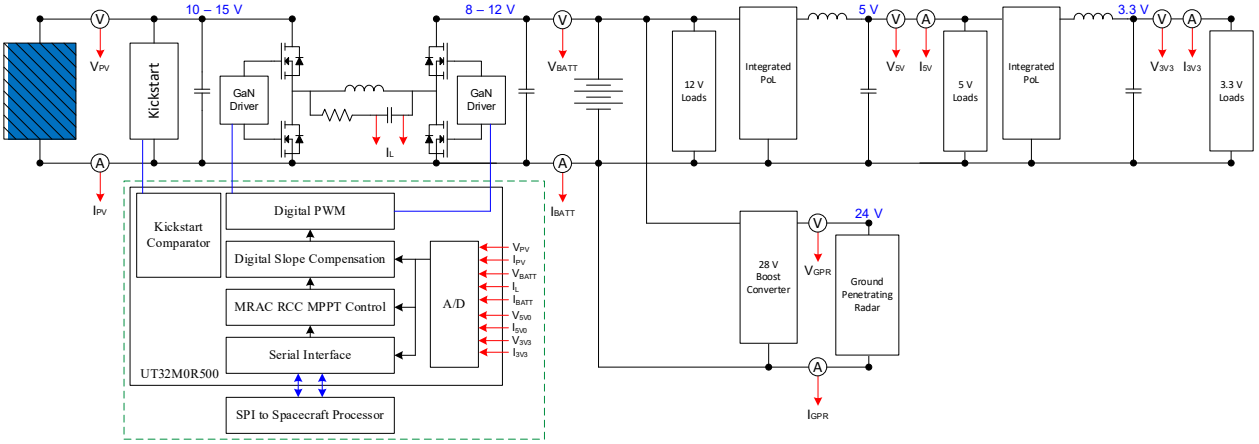

Figure 2. PUFFER Power Subsystem Architecture

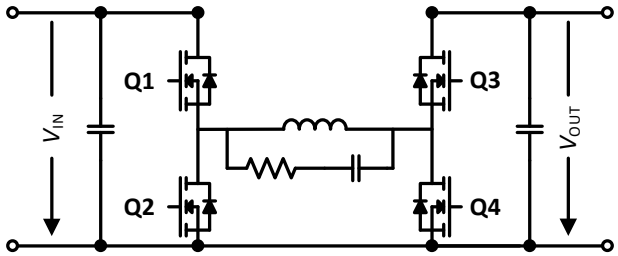

Figure 3. Buck-Boost Converter Topology

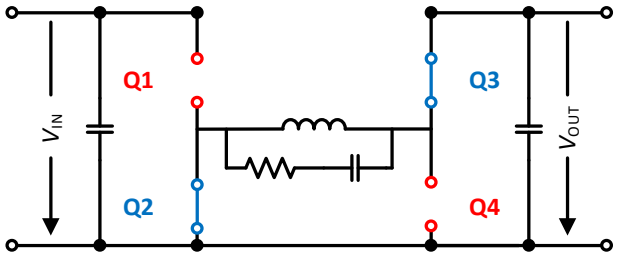

Figure 4. Boost Mode of Buck-Boost Topology

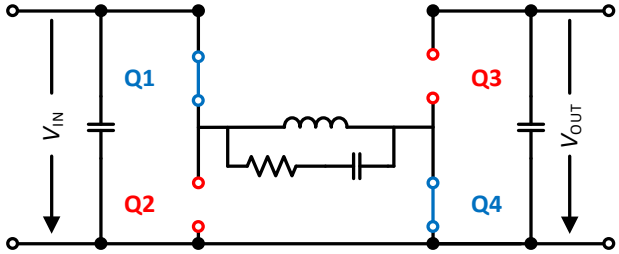

Figure 5. Buck Mode of Buck-Boost Topology

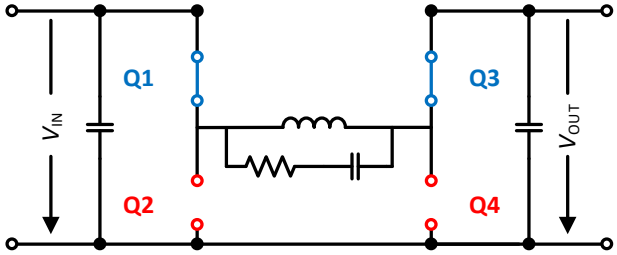

Figure 6. Pass Mode of Buck-Boost Topology

PHOTOVOLTAIC BUCK BOOST CONVERTER

In order to provide power from the photovoltaic (PV) array to the battery on PUFFER, a wide input range must be converted to an overlapping wide output range, requiring buck-boost operation in the solar array converter. To meet this need, a four-switch, non-inverting buck boost converter has been implemented using GaN FETs to achieve high efficiency across the input and output voltage ranges, the topology for which can be seen in Fig. 3. The non-inverting buck boost can provide good performance in either buck or boost mode, but traditionally experiences decreases in efficiency when utilized at unity gain, resulting from maximum conduction losses and a relative increase in switching losses as the converter toggles between buck and boost modes [4], [5]. Several approaches have been used in commercial applications to mitigate these losses, including mode-selection [6], sliding-mode control [7], and hysteretic current-mode control [4]. Hysteretic control minimizes switching and conduction losses in the converter, by introducing a pass state of the converter, resulting in a direct energy path from the solar array to the battery. This work takes advantage of this by implementing a modified hysteretic current-mode control through the addition of an additional MPPT outer control loop implemented through a ripple correlation control (RCC) algorithm, as described in [2]. The resulting control path is implemented digitally on a state machine built on the UT32M0R500 ARM M0+ Cortex Microcontroller [3] and is illustrated in Fig. 7.

To control the battery charging around the maximum power point (MPP) of the PV array, three separate control elements are used. First, a RCC MPPT algorithm is implemented. Based on that algorithm, the derivative of the input power is compared to the derivative of the inductor current. Based on the sign of the comparison, the reference voltage to the digital PID is increased or decreased, pushing the converter closer to the operating duty cycle to achieve MPP on the PV array. However, as described in [4], the reference is then passed to a hysteretic control algorithm, which selects switches based on the measured magnitude and sign of the inductor current. Based on that algorithm, the converter is switched into boost (Fig 4.) buck (Fig. 5), or pass (Fig. 6) state. The hysteretic windows for v_{IB}, v_{IM}, and v_{IT}, are determined based on the commanded v_C and the magntitude of expected inductor ripple, where:

$$v_{IB} = v_C, v_{IM} = v_C + \Delta v(I_L), \text{and } v_{IT} = v_C + 2\Delta v(I_L)$$

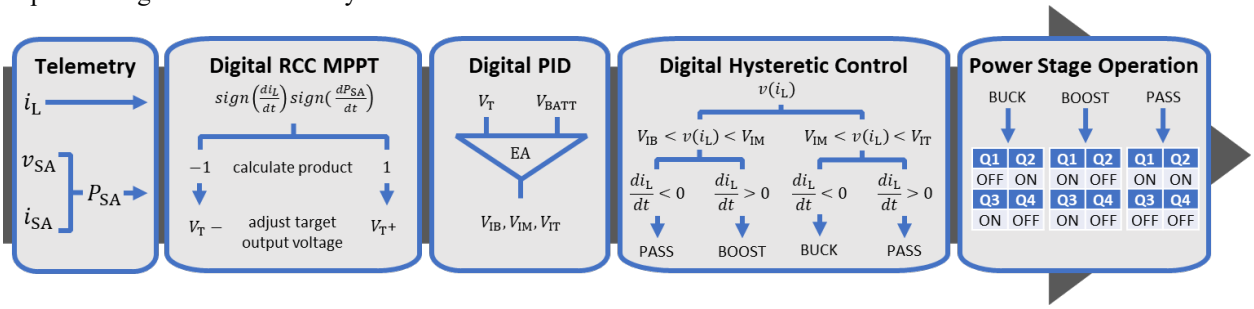

Figure 7. Control algorithm flow chart for RCC MPPT and hysteretic buck-boost control

By placing the converter into the PASS state when the derivative of the measured inductor current is properly signed for the desired operating point, two key benefits are achieved over traditional PWM algorithms. First, switching is stopped when the input and output voltages are equivalent, allowing for direct energy transfer to the battery without incurring switching losses. Further, variable frequency switching reduces the switching losses incurred in the converter when input and output do not match, resulting in an exceptionally efficient PV converter for its operating range.

Prototype PV Converter Demonstration

In order to demonstrate the techniques described in the previous section, a demonstration PV buck-boost converter was developed. The converter was sized for up to 250 W loads, but the technology is scalable to the load application, which will be discussed later in this work. To compare the PUFFER-optimized converter to the prototype, the parameters for each are provided in Table 2 and Table 3, respectively.

Table 2: PUFFER PV Converter Specifications

Parameter	Minimum	Maximum
Output Power	0 W	25 W
Input Voltage	10 V	15 V
Output Voltage	12 V	12 V
Output Current	0 A	3 A

Table 3: Prototype PV Converter Specifications

Parameter	Minimum	Maximum
Output Power	0 W	250 W
Input Voltage	22 V	100 V
Output Voltage	22 V	36 V
Output Current	0 A	12 A

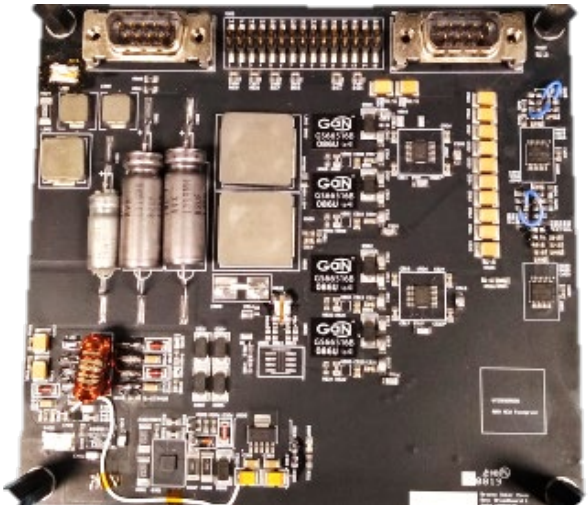

Figure 8. Prototype PV Buck-Boost Converter

The prototype, designed for higher solar array voltages up to 100 V, was optimized around load powers up to 250 W across its voltage range, and derated to operate across a full voltage rage from 22 V – 100V input and 22 V – 36 V output. The resulting component specifications for the prototype are shown in Table 4.

Table 4: Prototype PV Converter Components

Component Type	Part Number
Switching FETs	GS66516T
Inductors	SGIHLP60HEB6R8M81S
Bulk Input Capacitance	T550B756M075AH
Bulk Output Capacitance	T510X337K010CH641C
Microcontroller	UT32M0R500

As noted in [8], switch node referenced gate drivers that are TID tolerant do not exist at high voltages for conversion utilizing GaN HEMT devices in high radiation environments. To mitigate this, gate driving was for floating FETs was achieved using a scheme similar to that proposed in [9], combining a digital isolator, offline flyback converter, and low-side GaN driver, along with optimized gate drive impedance [10] to achieve rapid, safe turn-on of the GaN HEMTs under all load conditions. The power stage was optimized around a 1 MHz switching frequency, allowing the hysteretic controller to rapidly switch between control modes to provide efficient conversion, while minimizing filtering component sizing.

Based on these design considerations, a prototype of the PV buck-boost converter was fabricated as shown in Fig. 8. Laboratory testing was performed on the prototype unit for component-level evaluation and feed-forward into flight developments. The tested prototype performed well, achieving peak efficiencies of 95 % from solar array to bus when operating at its conversion ratio extreme of 4.5:1, as shown in Fig. 9.

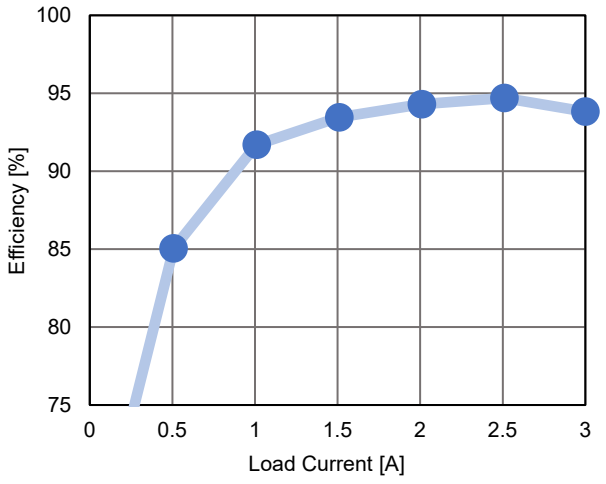

Figure 9. Measured PV Buck-Boost Efficiency

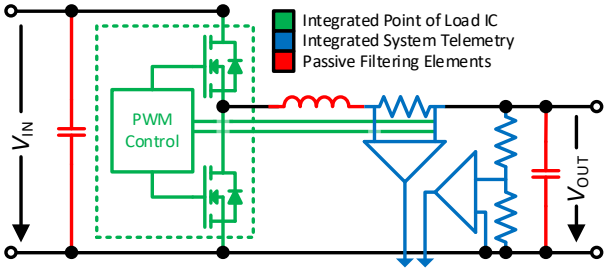

Figure 10. Integrated PoL buck converter

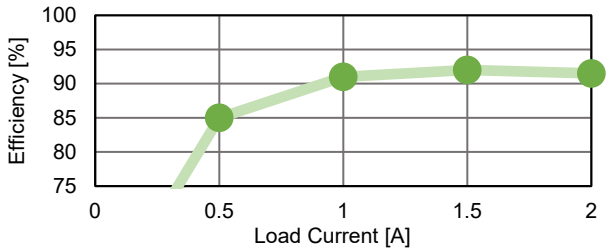

Figure 11. Simulated PoL buck converter efficiency

INTEGRATED POL BUCK CONVERTERS

Two PoL converters are needed for supplying the FPGA, microcontroller, and telemetry circuits on board PUFFER. In spacecraft applications, these converters tend to be bulky and inefficient, without providing housekeeping telemetry to the flight system. This development utilizes a FET-integrated PoL IC, along with compact discrete components and integrated telemetry collection for converter voltage and current that is communicated to the flight system via SPI for fault identification in case of a failure. The PoL system architecture is shown in Fig. 10 and the specification for the converter is shown in Table 5.

Table 5: Point of Load Converter Specification

Parameter	Minimum	Maximum
Output Power	0 W	10 W
Input Voltage	5 V	12 V
Output Voltage	3.3 V	5 V
Output Current	0 A	2 A

In Fig. 9, integrated elements in the converter's power stage are shown in ***green***, integrated elements in the telemetry system are shown in ***blue***, and passive elements are shown in ***red***. The designed module is easily scalable to various output voltages, and provides high efficiency to the load at conversion ratios up to 3.63:1. The efficiency for the module is shown for 12 V to 3.3 V conversion in Fig. 10, achieving peak efficiency of 92 % and full load efficiency of 91.5 %, with a modular design that can be utilized throughout the PUFFER platform for Lunar surface missions.

GPR BOOST CONVERTER

Of the multitude of potential instruments that are compatible with the PUFFER concept platform, a GPR can be used for multi-agent radar imagery of the Lunar surface. The proposed GPR unit requires an input of 24 V and 6 W, requiring boosted conversion from the low PV voltage on the PUFFER concept platform. To meet that need, a compact boost converter was designed, based around the RH3845 synchronous buck converter die and external GS61004B GaN FETs to achieve high efficiency at the low load points in the converter design. The boost converter architecture is shown in Fig. 12 and the specification for the converter is shown in Table 6.

Table 6: GPR Boost Converter Specification

Parameter	Minimum	Maximum
Output Power	0 W	100 W
Input Voltage	22 V	36 V
Output Voltage	0 V	30 V
Output Current	0.5 A	4 A

In Fig. 9, elements in the converter's power stage are shown in ***green***, integrated elements in the telemetry system are shown in ***blue***, and passive elements are shown in ***red***. Unlike the PoL converters described previously, the boost converter power stage is implemented using discrete components, but still provides high efficiency performance for conversion ratios up to 5:1. The efficiency for the GPR boost converter is shown for 8 V to 24 V conversion in Fig. 13, achieving peak efficiency of 92% and full load efficiency of 89 %, enabling efficient use of the compact GPR.

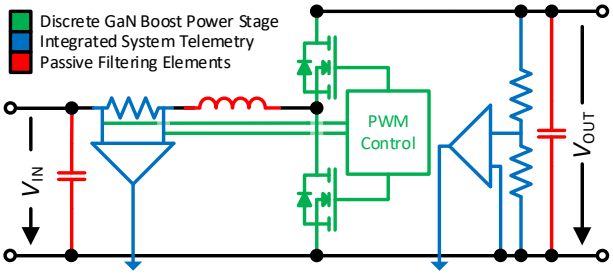

Fig. 12. GaN-Based GPR Boost Converter

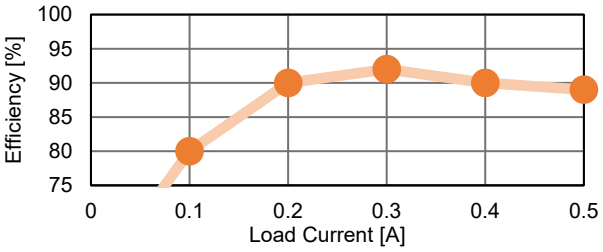

Fig. 13. Simulated GPR boost converter efficiency

PUFFER-OPTIMIZED IMPLEMENTATION

To optimize the converter design for the PUFFER mission concepts for the lunar surface, development is ongoing. Two implementation methods are shown in rendered model Fig. 14, with a single sided PCB designed for the complete power system in Fig. 14 (a) and a 3D-integrated flex PCB shown in Fig. 14 (b). The conversion stages achieve power density of 2 W/cm^3 power density, and the entire design fits within a 100 g mass allocation. They are designed to be directly integrated to an interface PCB on the PUFFER platform, allowing for rapid integration into functional and environmental PUFFER testbeds.

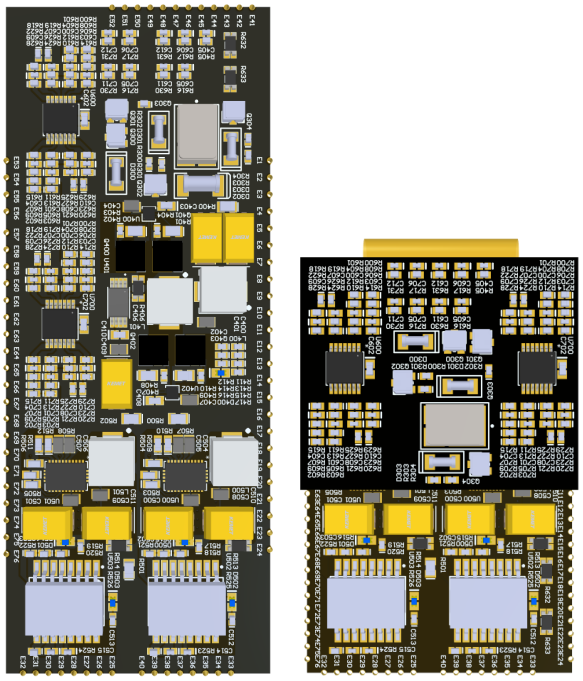

(a) (b)

Figure 14. PUFFER-optimized power system

CONCLUSION

This paper has presented the development of a power subsystem for the PUFFER robotic mobility system, focused on optimization for use in radiation environments including the Lunar and Martian surfaces. The power system introduces GaN-based converters for numerous applications, utilizes a combined RCC MPPT algorithm with a hysteretic controller to achieve 95 % efficient conversion from PV to battery, as well as distributed PoL and instrument converters to achieve greater than 90 % efficient conversion to all loads. development of the system. The resulting system provides a compact, lightweight, and efficient solution for the PUFFER platform, and will enable PUFFER and similar exploration platforms throughout the solar system.

ACKNOWLEDGEMENTS

The authors would like to acknowledge the programmatic support and contributions provided by Raphael Some (JPL) and Pat Beauchamp (JPL). This research was carried out at the Jet Propulsion Laboratory, California Institute of Technology, under a contract with the National Aeronautics and Space Administration and funded through the internal Research and Technology Development program.

REFERENCES

[1] Croix, J. P., Karras, J., “PUFFER: NASA’s Pop-Up Origami Rover”, Keck Institute for Space Studies, California Institute of Technology, 2019, available: https://www.kiss.caltech.edu/lectures/2019_PUFFER.html

[2] Khanna R., Zhang, Q., Stanchina, W. E., Reed, G. F., Mao, Z., "Maximum Power Point Tracking Using Model Reference Adaptive Control," IEEE Transactions on Power Electronics, vol. 29, no. 3, pp. 1490-1499, 2014.

[3] “UT32M0R50x 32-bit ARM Cortex-M0+ Microcontroller”, Cobham, 2017, available: https://scss.cobhamaes.com/pagesproduct/datasheets/UT32M0R500_Product-Brief.pdf

[4] Hong, X-E., Wu, J-F., Wei, C-L., “98.1%-Efficiency Hysteretic-Current-Mode Noninverting Buck–Boost DC-DC Converter With Smooth Mode Transition”, IEEE Transactions on Power Electronics, vol. 32, no. 3, pp. 2008-2017, 2017

[5] Sahu, B. and Rincon-Mora, G. A., "A low voltage, dynamic, noninverting, synchronous buck-boost converter for portable applications," in *IEEE Transactions on Power Electronics*, vol. 19, no. 2, pp. 443-452, March 2004

[6] Lee, Y., Khaligh, A., and Emadi, A., "A Compensation Technique for Smooth Transitions in a Noninverting Buck–Boost Converter," in *IEEE Transactions on Power Electronics*, vol. 24, no. 4, pp. 1002-1015, April 2009

[7] Wang, L., Meng, F., Sun, Z., Yang, S., and Yang, W., "An adaptive hysteresis sliding mode control method for double-switch buck-boost converter," *2017 IEEE Transportation Electrification Conference and Expo, Asia-Pacific (ITEC Asia-Pacific)*, Harbin, 2017

[8] Barchowsky, A., Amirahmadi, A., Stell, C., Merida, E., Bolotin, G., Ulloa-Severino, T., and Carr, G., "A Class of GaN-Based, Radiation-Hardened Power Electronics for Jovian Environments," in European Space Power Conference, Juan-les-Pins, France, 2019.

[9] Huang, X., “High Frequency GaN Characterization and Design Considerations”, Virginia Polytechnic Institute and State University, VA, 2016

[10] Barchowsky, A., Kozak, J. P., Hontz, M. R., Stanchina, W. M., Reed, G. F., Mao, Z. H., Khanna, R., "Analytical and experimental optimization of external gate resistance for safe rapid turn on of normally off GaN HFETs," *2017 IEEE Applied Power Electronics Conference and Exposition (APEC)*, Tampa, FL, 2017, pp. 1958-1963